

1 **An Exploratory Shockwave Approach for**
2 **Signalized Intersection Performance Measurements**
3 **Using Probe Trajectories**
4
5

6 Yang Cheng*
7 Graduate Research Assistant
8 Civil and Environmental Engineering
9 University of Wisconsin - Madison
10 Madison, WI 53706
11 Tel: 608-262-2524
12 Email: cheng8@wisc.edu
13

14 Xiao Qin, PhD, PE
15 Assistant Professor
16 Civil and Environmental Engineering
17 South Dakota State University
18 Brookings, SD 57007
19 Email: xiao.qin@sdstate.edu
20

21 Jing Jin
22 Graduate Researcher Assistant
23 Civil and Environmental Engineering
24 University of Wisconsin - Madison
25 Madison, WI 53706
26 Tel: 608-262-2524
27 Email: jjin2@wisc.edu
28

29 Bin Ran, Ph.D.
30 Professor
31 Civil and Environmental Engineering
32 University of Wisconsin - Madison
33 Madison, WI 53706
34 Tel: 608-262-0052
35 Email: bran@wisc.edu
36
37
38

39 Word Count: 6256+ 1 Tables * 250 + 8 Figures * 250 = 8506
40
41

42 * *Corresponding Author*

1 **ABSTRACT**

2 An innovative approach for arterial intersection performance measurement using vehicle
3 trajectory data is proposed in this paper. The vehicle trajectories are first processed to
4 extract the points representing the changing vehicle dynamics, which are named the
5 “critical points” on the trajectory. The extraction technology can also be used as a data
6 reduction method in on-vehicle devices to reduce the communication cost. A shockwave
7 based method then uses the critical points to detect the signal timing, providing a basis
8 for real time performance measurement. A cycle-by-cycle queue length estimation
9 method is also proposed as a case study of signalized intersection performance
10 measurement. The performance of this approach is tested both by simulation and NGSIM
11 trajectory data. The results indicate that this trajectory based approach is promising.
12

1 INTRODUCTION

2 Arterial performance measurements are essential for advanced traffic management
3 systems (ATMS) and advanced traveler information systems (ATIS). Although nearly
4 40% of the nation's vehicle miles traveled (VMT) occur on arterials, real-time arterial
5 performance measurement systems are not as mature as their freeway counterparts. Two
6 of the biggest challenges are: 1) arterial traffic conditions are more complicated than the
7 ones on freeways because of the periodic interruptions from traffic signals, random
8 friction from crossing traffic on minor streets, driveway related activities, etc; 2) the
9 current traffic collection technologies deployed on arterials are not sufficient for
10 measuring real-time operational performance(1).

11 Given these challenges, recent research development is focused on two areas: 1)
12 modeling the relationship performance measures (such as travel time, delay, queue
13 length) and traffic flow as well as signal timing; and 2) developing new data collection
14 technologies or using new data sources (1-3) . For example, in the first area, arterial
15 travel time or delay is modeled as the function of occupancy, flow, speed and/or signal
16 timing parameters. Usually, regression methods are used to calibrate these parameters to
17 obtain the best goodness of fit (4-6). These models are usually site-specific, which limits
18 the transferability for different prevailing traffic conditions, signal control and
19 intersection geometries. One of the improved solutions proposed by Xie et al (7) used
20 calibration-free parameters, which decomposed the travel time into cruise time and signal
21 delay. Cruise time was the running time calculated using detected speed via inductive
22 loop detectors and signal delay was calculated by a simplified Webster formula.
23 Skabardonis and Geroliminis (8) proposed an analytical model using inductive loop
24 detector data (aggregated in 20 or 30 seconds) and signal timing, which carefully
25 calculates the delay as the sum of signal delay, queuing delay and oversaturation delay.
26 An important improvement is that their model addressed the cases when the queue is
27 longer than the distance from the loop detector to the stop bar. By the same token but
28 with different methodologies, other works uses stochastic theories (9, 10), or artificial
29 intelligence (AI) methods (11, 12). Growing interests in the second area develop along
30 with the emerging and advancement of traffic signal and probe technologies with which
31 new data sources or high resolution data such as the timestamps for individual vehicle
32 arrival (1, 3, 13), vehicle re-identification technologies (14-17), and probe data (18-23)
33 become readily available.

34 In most current studies, vehicle re-identification and probe data are only used to
35 generate sample travel times between points which are subsequently modeled in a
36 statistical sampling domain (18-21). The sample rate requirement was discussed (24).
37 Some of the reasons for this type of application are: 1) general automatic vehicle
38 identification (AVI) technologies, such as toll tag, automation license plate match,
39 vehicle re-identification, can only provide travel times between two pre-defined points; 2)
40 some automatic vehicle location (AVL) devices have relatively long sampling intervals,
41 such as 1 minute, which makes it impossible to obtain vehicle trajectories from the
42 scattered points.

43 The development of traffic detection technologies makes the utilization of probe
44 vehicle trajectory data possible. There are some studies about using trajectories of the
45 total vehicle population for shockwave identification and analysis. The work of Lu and
46 Skabardonis (25) studied the "local minima" in the speed domain of the trajectory and

1 used the “local minima” to analyze the back propagating shockwaves caused by
2 congestion. Izadpanah et al (26) modeled the actual trajectories in the distance domain as
3 a piece-linear line and defined “joint point” (major shockwave intersection points) at the
4 trajectory. An iterative two-phase piecewise regression was employed to extract joint
5 points from a trajectory. “Joint points” were used to detect the major shockwaves and
6 their speed. There are also a few attempts of using vehicle trajectories for performance
7 measurements (2, 27). The detailed trajectory data can provide more abundant and
8 detailed traffic information than simple travel times between two ends of a pre-defined
9 route, especially for the interrupted and discontinuous traffic flow on arterials. More
10 importantly, congestion can be easily detected using trajectory data because unusually
11 low speeds and frequent stops can be detected directly. Conversely, the number of
12 available sampled travel times would drastically decrease due to a low flow rate and the
13 responding time (assuming real time) will dramatically increase because the sampled
14 travel will only be available after the probe vehicle finishes the pre-specified route.
15 However, the main challenge of developing a trajectory-based model is how to convert
16 the microscopic detections into macroscopic performance measurements, which is not as
17 straightforward as sampling travel time. One trajectory only represents the individual
18 behavior of one vehicle, which is often subject to actual situations encountered by the
19 driver. Therefore the data are more volatile. On the contrary, arterial performance
20 measures should be macroscopic and easily understood such as average travel time and
21 maximum queue length. Recent attempts of performance measurements using probe
22 trajectory include the research conducted by Claudel et al (27). In their study, the probe
23 trajectory measurement was converted to density estimation using the Moskowitz
24 function (28, 29) for freeway travel time estimation. The trajectories of probes on
25 signalized arterials are more complicated than freeways because of the periodic
26 turbulence due to signals and local friction. Comer and Cetin (18) studies the conditional
27 probability distribution of the queue length at an isolated intersection given the locations
28 of probe vehicles in the queue. They found that only the location of the last probe in the
29 queue is necessary for queue length estimation, however, the assumption that the actual
30 percentage of probe vehicles among the traffic stream is known limits the applications of
31 this method.

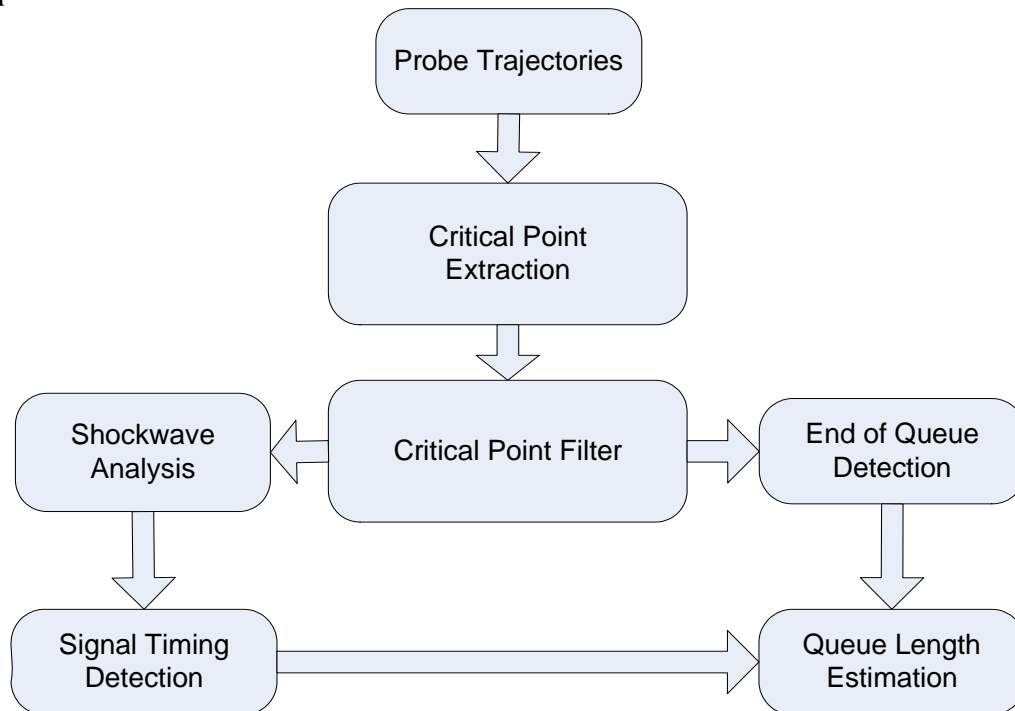
32 The existing work related to arterial trajectory data has not really led to practical
33 applications of providing useful information such as queue length and travel time. This
34 paper explores the feasibility of using the vehicle trajectory data for intersection
35 performance measurement. The proposed approach first defined the critical points (CPs)
36 on a trajectory which are able to capture the dynamics of the vehicular movement in a
37 space-time diagram. A method was developed to extract the CPs and then shockwave
38 based methods were used to detect signal timing and to estimate the cycle-by-cycle queue
39 length. The theories were tested by numeric experiment using both simulation data and
40 real trajectory data from NGSIM. The paper is concluded with an overview of the study
41 and a discussion of future studies.

42

43 **METHODOLOGY**

44 Given the intersection and link geometric characteristics, the intent is to develop a real-
45 time intersection performance estimation model using vehicle trajectory data as the only
46 model input. Figure 1 shows the overall building blocks for the methodology as well as

1 the relationship between them. The workflow can be described as follows: “Critical Point
 2 Extraction” module first processes the real-time trajectories to generate a series of CPs;
 3 the “Critical Points Filter” module selects part of the generated CPs for different
 4 purposes; using shockwave speed, the signal timing can be detected and determined; and
 5 finally the maximum queue length in a cycle can be estimated based on the detected end
 6 of queue.



7
 8
 9
 10
 11
 12
 13
 14
 15
 16
 17
 18
 19
 20
 21
 22
 23
 24
 25
 FIGURE 1 Methodology Flow Chart

10 Modeling Trajectories

11 The trajectory of a vehicle can be described as a series of points, $\{x_t\}$, where x_t is a record
 12 of the vehicle at time t . x_t is a vector and describes the dynamics of vehicle at time t ;
 13 $x_t = [l, v, a]$, where l is the location, v is the speed and a is the acceleration rate. l , v and
 14 a represent the three dynamic features.

15 The movements of vehicle are not totally random; drivers can be assumed rational
 16 and they fulfill three major tasks: 1) maintain a desired speed; 2) keep a safe distance
 17 from the lead vehicle; 3) follow the signal indication. For instance, when a vehicle travels
 18 in a platoon on a well coordinated corridor, it travels at a near constant speed and its
 19 trajectory is already known given the start point x_{t_0} and the speed v_0 , where t_0 is the start
 20 of time. For a general case, the trajectory of a vehicle can be divided into several regimes
 21 which are either uniform motion or uniformly accelerated motion. Therefore, critical
 22 points (CPs), $\{x_t^c\}$, which are a subset of $\{x_t\}$ can be defined. These CPs correspond to
 23 changing points on the borders of the movement regimes. Therefore, “non-critical” points
 24 become redundant and the trajectory $\{x_t\}$ can be reduced to a set of CPs $\{x_t^c\}$, as shown
 25 in Figure 2.

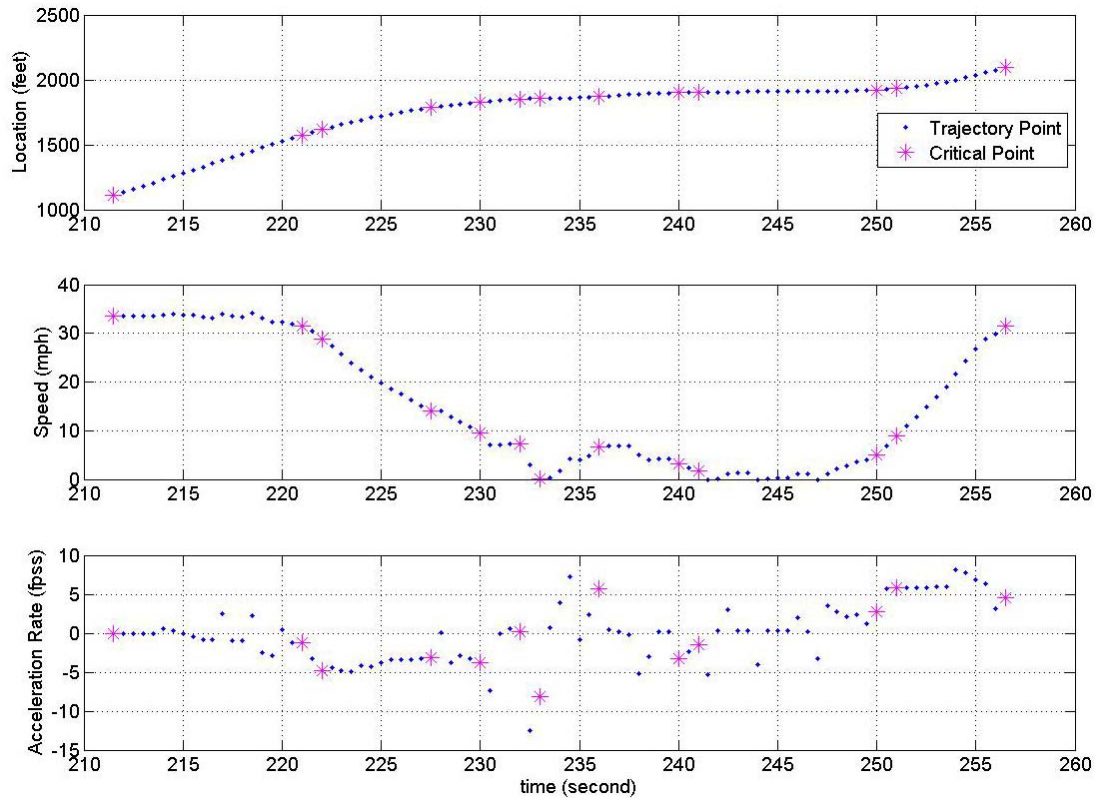


FIGURE 2 CPs at a Trajectory (Paramics Simulation Data)

($c_v = 3\text{mph}$, $c_a = 3\text{fpss}$, $c_{v,stop} = 3\text{mph}$ See next section)

1
2
3
4
5
6
7
8
9
10
11
12
13
14
15
16
17
18
19
20
21
22
23
24

For the purpose of traffic detection, CPs result from the changes in traffic conditions, significant and trivial. For example, the CP from slowing down to speeding up indicates the distance headway is increased, resulting from a queue clearance. Some CPs correspond to local traffic turbulence and . Hence, the features of the critical points can be used for signalized intersection performance estimation, which will be presented in detail in the following sections.

In the above analysis, lane changing is not explicitly discussed. In fact, for simplicity, the vehicles are assumed to travel on a one-dimensional road. Note that the trajectory modeling approach can be easily extended to two-dimension by defining the current traveling lane as the fourth dynamic feature besides location, speed and acceleration rate.

It is also interesting to treat the trajectories from the view of information science as a signal serial. A new CP extraction algorithm could be developed by borrowing data compression ideas. Converting $\{x_t\}$ to $\{x^c_t\}$ is analogous to “data reduction”, which has another benefit for the real-time floating car data (FCD) collection by reducing data to be transmitted. If the onboard device has a CP extraction program running, the real-time data uploaded would be CPs. Therefore the communication cost is reduced. Obviously, this approach has advantages over the current probe measurement technologies which record at a fixed time interval.

1 **Critical Points Extraction**

2 As analyzed above, the main idea of CP extraction is that the movement of a vehicle
3 between two CPs is definitive and belongs to one of the two basic movements: 1)
4 uniform motion; 2) uniformly accelerated motion (the acceleration rate is negative for
5 deceleration motion). Therefore, a trajectory can be divided into several regimes with
6 CPs as the boundaries. The extraction of a CP can be formulated as:

7 Find $\max(n)$, when Equation (1) or (2) is satisfied for all the:

8 if $|a_i| < c_a$,

$$9 \quad \left| \tilde{v} - v_i \right| < c_v \quad (1)$$

10 or, if $|a_i| \geq c_a$,

$$11 \quad \left| \tilde{a} - a_i \right| < c_a \quad (2)$$

12 Where \tilde{v} is the median speed of $\{x_i\}$, c_v is a threshold, \tilde{a} is the median acceleration rate of
13 $\{x_i\}, i=1,2\dots n$, c_a is a threshold, x_1 the previous CP or the first point on the trajectory.
14 Eq. (1) represents the uniform motion and Eq. (2) represents uniformly accelerated
15 motion.

16 In addition, considering the end of queue detection, it is necessary to treat
17 stopping or very low speed as a special case; otherwise, the actual point when and where
18 the vehicle joins the standing queue might be missed:

$$19 \quad |v_i| < c_{v,stop} \quad (3)$$

20 The CP extraction algorithm can be summarized as: given the consecutive feeding
21 of trajectory points, one of Eq. (1) and (2) will be applied according to whose condition is
22 satisfied; however, if Eq. (3) satisfies, it overrides, continuing to search the following
23 “stopping” segment and put down the first and last as CPs and then Eq. (1) and (2) apply
24 again.

25 The selection of thresholds would not be affected by traffic or geometric
26 conditions since CPs are intended to be the “change” points on a vehicle trajectory; that
27 is, CPs are the associated directly with vehicle dynamics. As long as how detailed the
28 dynamics needed to be known is determined, the thresholds are determined. The *Travel*
29 *Time Data Collection Handbook* (30) mentions that “typically” less than 5 mph can be
30 considered as stopping; it was found that lower threshold, could locate the point when the
31 vehicle join the standing queue more accurately, which shall benefit the selection of Type
32 II CP in the next section, As for the thresholds of speed and acceleration rate, c_v and c_a ,
33 it is found that smaller values of thresholds would produce more CPs; however, the
34 selected Type I, II and III CPs afterwards (in the next section) usually have very small
35 shifts in the location and time. In the *Numeric Experiment* section, $c_v = 3mph$,
36 $c_a = 3fps$ and $c_{v,stop} = 3mph$.

1 An example is shown by Figure 2, where an entire trajectory is processed and the
2 generated CPs are marked. As mentioned in the Introduction, there are a few studies in
3 identifying and analyzing shockwaves using vehicle trajectories, such as the work by Lu
4 and Skabardonis (25) and by Izadpanah et al. (26). The CP defined in this paper share
5 similarities with and “joint points” in but also have significant differences:

6
7 1. Assumptions are different

8 The CP in this paper is used to extract the movement changing at the trajectory while
9 “joint point” and “local minima” are for detecting “major shockwaves”. It can almost
10 be certain that for arterials, the “joint points” are a subset of the CPs for the same
11 trajectory. In a word, CP is for a sampled probe approach while “local minima” and
12 “joint points” are not.

13 2. Extraction algorithms are different

14 Given the different assumptions, the CP extraction algorithm proposed in this paper is
15 simple for real-time implementation with lower computational cost. “Local minima”
16 method searches the local minimal speed points within a time window and “joint
17 point” method uses an iterative two-phase piecewise regression model for the location
18 domain. Although generated CPs tend to be noisier, setting proper thresholds and a
19 well designed “Selection of Critical Points” module can reduce the harmful noise to a
20 minimum.

21 3. Potential applications are different

22 Our algorithm can also be used as a data reduction method in the onboard GPS device
23 to reduce the communication cost without cost of traffic detection. In addition,
24 although CPs tend to be noisier, they may also include useful details about how speed
25 changes which could be valuable for other researches such as emission and safety
26 studies.

27
28
29
30 **Critical Points Filter for Various Purposes**

31 For different applications, different parts of the extracted CPs should be used. In other
32 words, a filter should be applied to choose the appropriate CPs. For example, when
33 critical points are used for signal detection, only the critical points which result from
34 signal changes should be used.

35 Figure 3 demonstrates the three types of CPs which will be referred in the
36 following discussion. Type I is defined as the CP which is the beginning point of a
37 deceleration regime caused by signal light turning to red; Type II is defined as the CP
38 which is the point when the vehicle slows down and joins the queue; Type III is defined
39 as the CP which is the beginning point of an acceleration regime caused by signal light
40 turning to green.

41

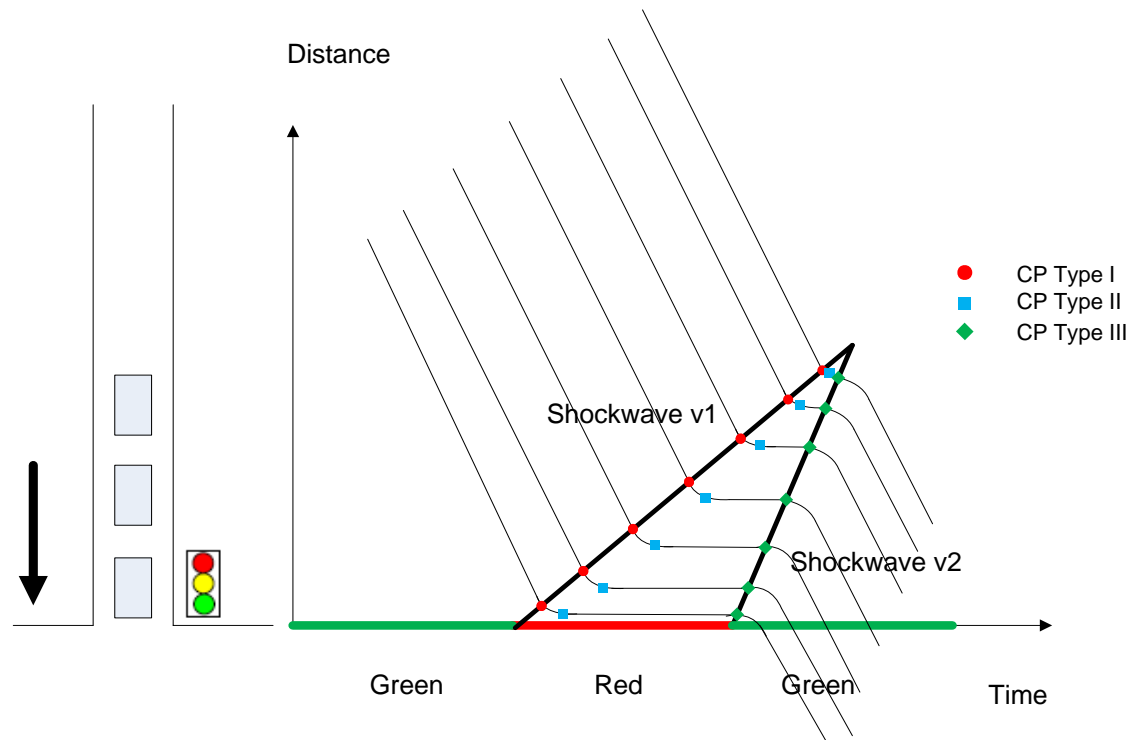


FIGURE 3 Shockwaves and Critical Points (CP)

The three types of CPs are selected from the whole extracted CPs by the features of CPs. These features are: 1) the time difference; and 2) the speed difference. The algorithm can be described as:

- (a) Order all the CPs from this vehicle chronologically and find the min speed CPs (index $j_1, j_2 \dots j_m$) with speeds less than $c_{v,stop}$; if no such CP exist, this vehicle is not stopped by a standing queue, and Type II and Type III CPs do not exist in the current trajectory.
- (b) Let $p = j_1$, find the first CP whose speed is less than its immediate previous CP with index of i ; if the speed of CP i is higher than all the CPs from i to j , i is the Type I CP and go to (c); if not, throw away the CP from first to i , do this step again;
- (c) CP j_m is the Type II CP; CP $j_m + 1$ is the Type III CP.

For simplicity, the above algorithm does not consider the case that the probe could not pass the intersection within a cycle. In that case, the trajectory has one than one stable stopping segments and the time differences (can be defined as center to center time difference) between them are comparable to the cycle length. One needs to divide the trajectory into segments using the max speed points between two consecutive stopping segments and apply the CP extract and filtering algorithms for each segment.

Figure 4 shows the selected Type I, II and II CPs from the generated CPs.

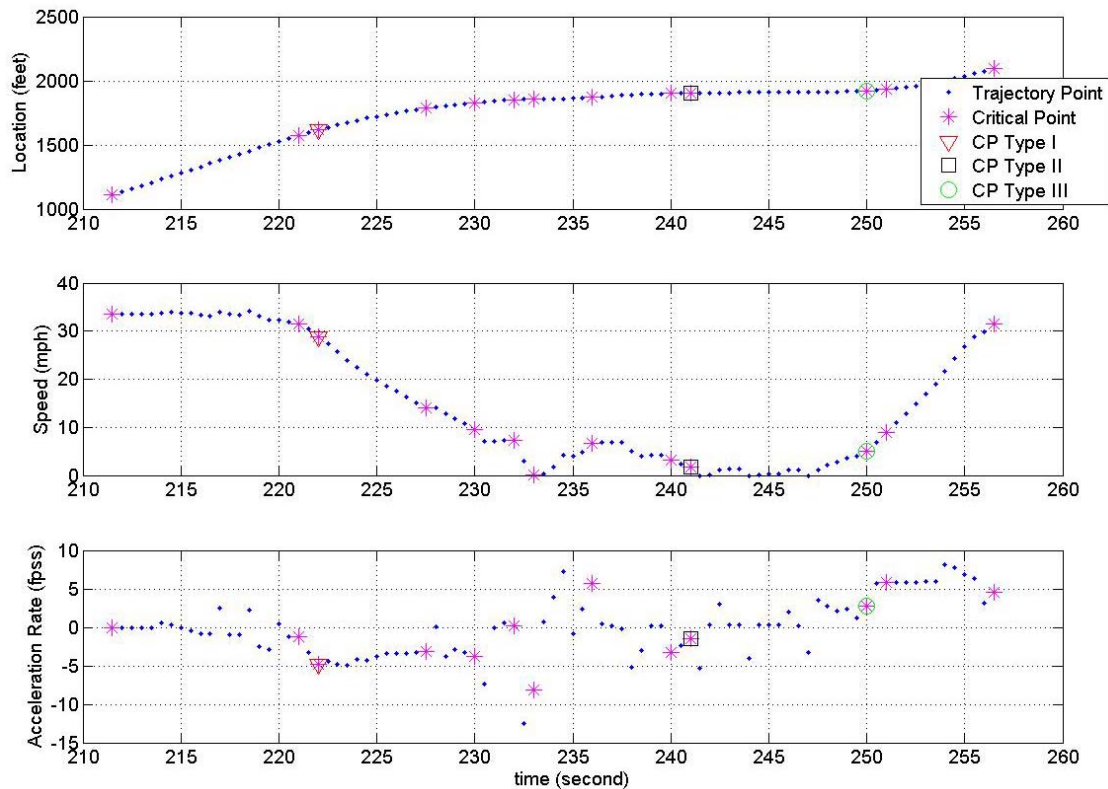


FIGURE 4 CPs and the Selected CPs for Further Applications at a Trajectory
(Paramics Simulation Data)

Signal Timing Detection

Signal timing is the major factor which affects the travel time on signalized arterials. Most studies related to arterial travel times use signal timing as input for their models (6, 7, 31, 32). However, real-time signal timing is not always available for online or even offline operations. According to the *2007 National Traffic Signal Report Card* (33), “Traffic Monitoring and Data Collection” received a score of F and “almost half of agencies (43 percent) reported having little to no regular, ongoing program for collecting and analyzing traffic data for signal timing.” Ban et al. explored the methods to derive signal timing using the delay measurements by Virtual Trip Line (VTL) technology based on GPS-equipped cell phones(34). Using sampled travel times, they found that a 40% penetration rate of probe was needed in order to obtain reliable signal timing detection. Below, we are going to demonstrate that the use of trajectory data can help detect signal timing data with a lower sample rate than only using sampled travel times.

The formation and dissipation of the queue before a stop-bar at signal changes cause vehicle movement changes which are then extracted as CPs. The time of the shockwaves caused by signal changes traveling to a vehicle is essentially the corresponding CP’s timestamp after the traffic light change. That being said, the signal timing parameters such as cycle length and green time can be obtained.

The fundamental and most widely used traffic flow model is the Lighthill-Whitham-Richards (LWR) model (35-37). The solution of LWR model is based on the

1 conservation equation of the traffic flow and a function of speed, flow (or density). The
 2 propagation speed of a shockwave is calculated as:

$$3 \quad v = \frac{q_u - q_d}{k_u - k_d} \quad (4)$$

4 Where,

5 q_u, q_d are the flow rate for upstream and downstream, respectively, and

6 k_u, k_d are the density for upstream and downstream, respectively.

7

8 As demonstrated in Figure 3 and 4, since the location and time of CPs are known
 9 from the trajectories, the start times of green time and red time can be detected as long as
 10 the shockwaves speeds can be estimated.

11 After the start of green, the queue accumulated before the stop bar starts to
 12 discharge. Therefore, the start time of the green light can be calculated as:

$$13 \quad T_g = T_{CP3}^* - \frac{L_{CP3}^*}{v_{dis}} \quad (5)$$

14 Where,

15 T_{CP3}^* is the adjusted time stamp of the Type III CP, ($T_{CP3}^* = T_{CP3} - v_{CP3} / a_{CP3}$, T_{CP3} is the
 16 time stamp of the Type III CP, v_{CP3}, a_{CP3} are the speed and acceleration rate of this Type
 17 III CP),

18 L_{CP3}^* is the adjusted distance of a Type III CP to the stop-bar ($L_{CP3}^* = L_{CP3} + v_{CP3}^2 / 2a_{CP3}$,

19 L_{CP3} is the time stamp of the Type III CP), and

20 v_{dis} is the queue discharge shock wave speed.

21

22 At the beginning of a green light, assume there is no queue spillback at the
 23 downstream intersection, the queue discharges at the saturation flow rate. The queue
 24 discharge shock wave speed can be estimated as:

$$25 \quad v_{dis} = \frac{q_s - 0}{k_m - k_j} \quad (6)$$

26 Where

27 q_s is the saturation flow rate,

28 k_m is the saturation flow density, and

29 k_j is the jam density

30 In the *Numeric Experiment*, $v_{dis} = 15\text{mph}$ was used.

31

32 After the start of red, traffic is stopped before the stop bar and the queue is
 33 formed. Therefore, the start time of the red light can be obtained by:

$$T_r = T_{CP1}^* - \frac{L_{CP1}^*}{v_{form}} \quad (7)$$

2 Where

3 T_{CP1}^* is the adjusted time stamp of the Type I CP, ($T_{CP1}^* = T_{CP1} - c_v / |a_{CP1}|$), T_{CP1} is the time
4 stamp of the Type I CP, a_{CP1} are the speed and acceleration rate of this Type I CP),

5 L_{CP1}^* is adjusted distance of Type I CP to stop-bar, $L_{CP1}^* = L_{CP1} + (2v_{CP1} + c_v)c_v / 2|a_{CP1}|$,

6 v_{CP1} is the speed of the Type I CP, L_{CP1} is the time stamp of the Type I CP), and

7 v_{form} is the queue formation shock wave speed.

8

9 The queue formation shockwave can be estimated as:

$$v_{form} = \frac{0 - q_u}{k_j - k_u} \quad (8)$$

11 Where

12 q_u is the upstream arrival flow rate,

13 k_u is the upstream arrival density, and

14 k_j is the jam density.

15

16 The problem now becomes how to get q_u and k_u . Using the basic flow-speed-
17 density relationship $q = kv$, either q_u or k_u can be determined by the other because the
18 inflow speed can be estimated by the vehicle speed before deceleration. There is no direct
19 way to estimate k_u or q_u , but the average density $\overline{k_{CP1}}$ from the stop bar to the Type I CP
20 can be estimated: assuming lane changing is limited when vehicles begin to slow and join
21 the queue, the number of vehicles before the probe vehicle can be accurately estimated
22 from dividing the distance from the Type II CP to the stop-bar by:

$$\overline{k_{CP1}} = \frac{L_{CP2}}{L_{CP1}} k_j \quad (9)$$

24 Where

25 L_{CP2} is the distance of the Type II CP from the stop-bar.

26

27 Therefore, Equation (8) is re-written and approximated as:

$$v_{form} = \frac{0 - q_u}{k_j - \overline{k_{CP1}}} = -\frac{q_u / \overline{k_{CP1}}}{k_j / \overline{k_{CP1}} - 1} \approx -\frac{v_{CP1}}{L_{CP1} / L_{CP2} - 1} \quad (10)$$

29 Where

30 v_{CP1} is the speed of the Type I CP.

1 **Dynamic Queue Length Estimation**

2 *End of the Queue Detection*

3 The detection of the end of the queue means the detection of an instantaneous queue
4 length. Some CPs correspond to the time and location when the vehicle joins the queue.
5 As discussed, Type II CPs are used.

6 7 *Maximum Queue Length Estimation during a Cycle*

8 The progress of queue formation and dissipation is greatly affected by the arrival pattern.
9 For an isolated intersection, the arrival flow rate within a cycle can be assumed to be
10 constant. Therefore, the queue length increasing rate can be calculated using the detected
11 end of queue and its timestamp. Given the already detected signal timing, the maximum
12 queue length can be calculated as:

$$13 \quad L_q = \frac{q_s q_u (T_g - T_r)}{k_j (q_s - q_u)} \quad (11)$$

14 The upstream arrival rate q_u can be estimated as:

$$15 \quad q_u = \frac{L_{CP2}}{k_j (T_{CP2} - T_r)} \quad (12)$$

16 Where,

17 L_{CP2} is the distance from the Type II CP to the stop-bar, and

18 T_{CP2} is the timestamp of the Type II CP.

19
20 Equation (11) is used for cases without an initial queue. Considering there are
21 stopped vehicles from the previous cycle, initial queue should be detected first and then
22 the total queue length can be estimated. The following formula can help to detect initial
23 queues:

$$24 \quad q_s (T_{CP2} - T_r) > L_{CP2} k_j \quad (13)$$

25 If Equation (13) does not satisfy, the initial queue is detected and the length of the
26 initial queue can be estimated by:

$$27 \quad L_{q0} = L_{CP2} - (T_{CP2} - T_r) q_s / k_j \quad (14)$$

28 For an intersection affected by an upstream signal, such as coordination, the
29 arrival pattern varies within a cycle because of the “gating effect”. The flow pattern from
30 upstream crossing streets may be significantly different from the main direction. The
31 resulting queue formation process is a complex process. As an approximation, the queue
32 increase process is modeled as a piecewise linear line. More than one Type II CPs are
33 needed for this case. Assume there are $n-1$ available Type II CPs, and use the point of
34 start of red as additional point (with the distance to stopbar is zero), order them
35 chronologically as a list of points on the queue length and time plane.

1 The average queue increase rate between each two consecutive points can be
 2 calculated as:

3
$$q_i = \frac{L_{CP2,i+1} - L_{CP2,i}}{T_{CP2,i+1} - T_{CP2,i}} \quad (15)$$

4 Where

5 i is the index, $i \in \{1, 2, \dots, n\}$,

6 $L_{CP2,i}$ is the distance from the i th Type II CP to the stop-bar, and

7 $T_{CP2,i}$ is the timestamp of the i th Type II CP.

8 Then several queue length estimates can be obtained:

9

10
$$\begin{aligned} L_{\max} &= L_{CP2,n} + q_{\max} t_{inflow} \\ L_{\text{last}} &= L_{CP2,n} + q_{n-1} t_{inflow} \\ L_{\min} &= L_{CP2,n} \end{aligned} \quad (16)$$

11 Where

12 $L_{\max}, L_{\min}, L_{\text{last}}$ are the three queue length estimates which use the max queue increase rate,
 13 the last available queue increase rate, and no queue increase, respectively,

14 $q_{\max} = \max(q_i)$, and

15 $t_{g,n}$ is the time duration from the n th Type II CP to the green light shockwave, and is

16 calculated by: $t_{g,n} = \frac{L_{CP2,n}}{v_{dis}} + t_g - T_{CP2,n}$ (see Figure (5), and note that the line of the queue

17 dissipation shockwave is: $y = v_{dis}(x - t_g)$).

Queue Length

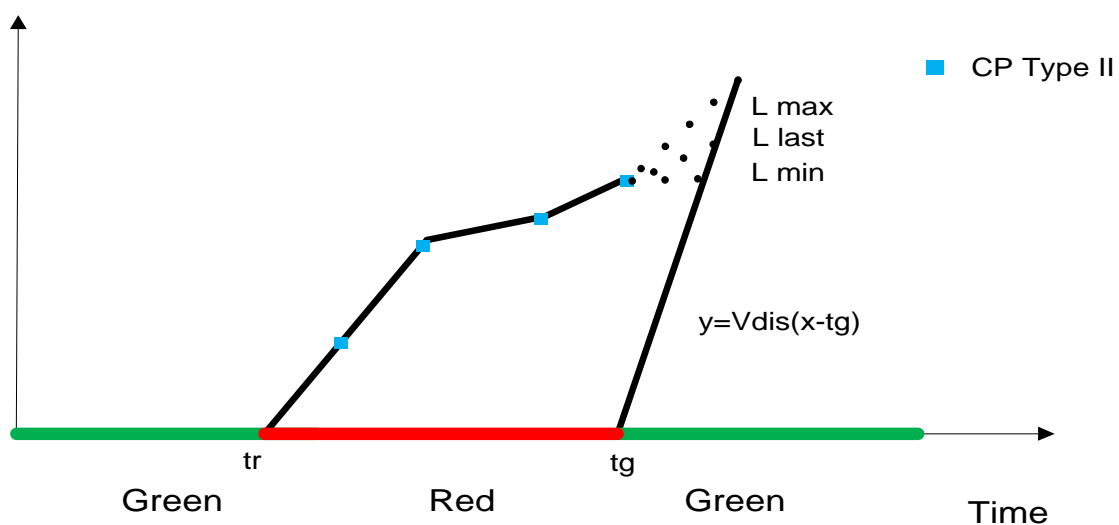


FIGURE 5 Queue Formation in Various Arrival Rates

18
 19
 20

1 The queue length of the cycle can be estimated as a weighted average:

$$2 \quad L_q = w_1 L_{\max} + w_2 L_{\text{last}} + w_3 L_{\min} \quad (17)$$

3 Where

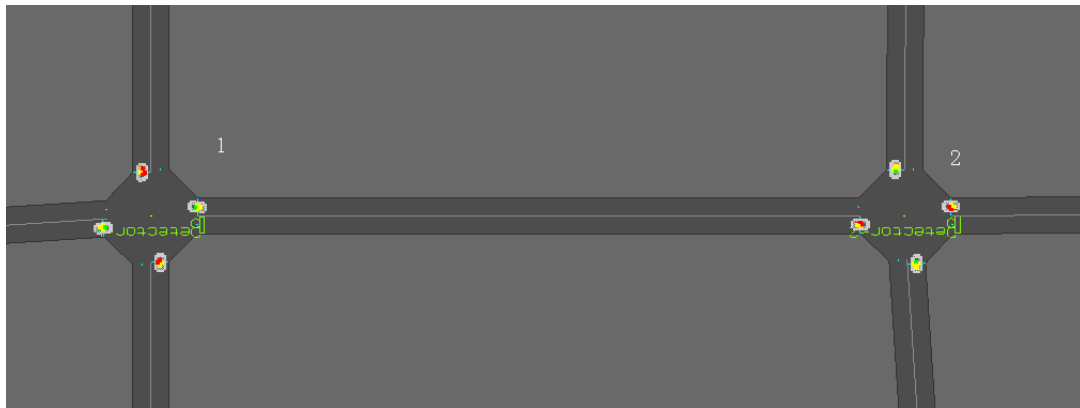
4 w_1, w_2, w_3 are the weights and $w_1 + w_2 + w_3 = 1; w_1, w_2, w_3 \in [0,1]$. In the *Numeric*
 5 *Experiment*, $w_2 = w_3$ and $w_1 = t_{g,n} / (t_{g,\max} + 2t_{g,n})$ ($t_{g,\max}$ is the time duration from the end
 6 Type II CP on the segment where the max queue increase rate is achieved.)

7 Note that the proposed models above are based on the critical points on a single
 8 trajectory excepted queue length estimation under various arrival rates, which implies
 9 low sample rate requirement. Model improvement for various sample rates and sensitivity
 10 analysis of the sample rate impact to models are beyond the scope of this paper, and are
 11 part of further work.

12 NUMERICAL EXPERIMENT

13 Data Source

14 There are two types of data used in this paper. One is a simulation network by Paramics
 15 (Figure 6) and the other is a trajectory data set from NGSIM((38)). The Paramics network
 16 is built as follows:



17 FIGURE 6 Paramics Simulation Network

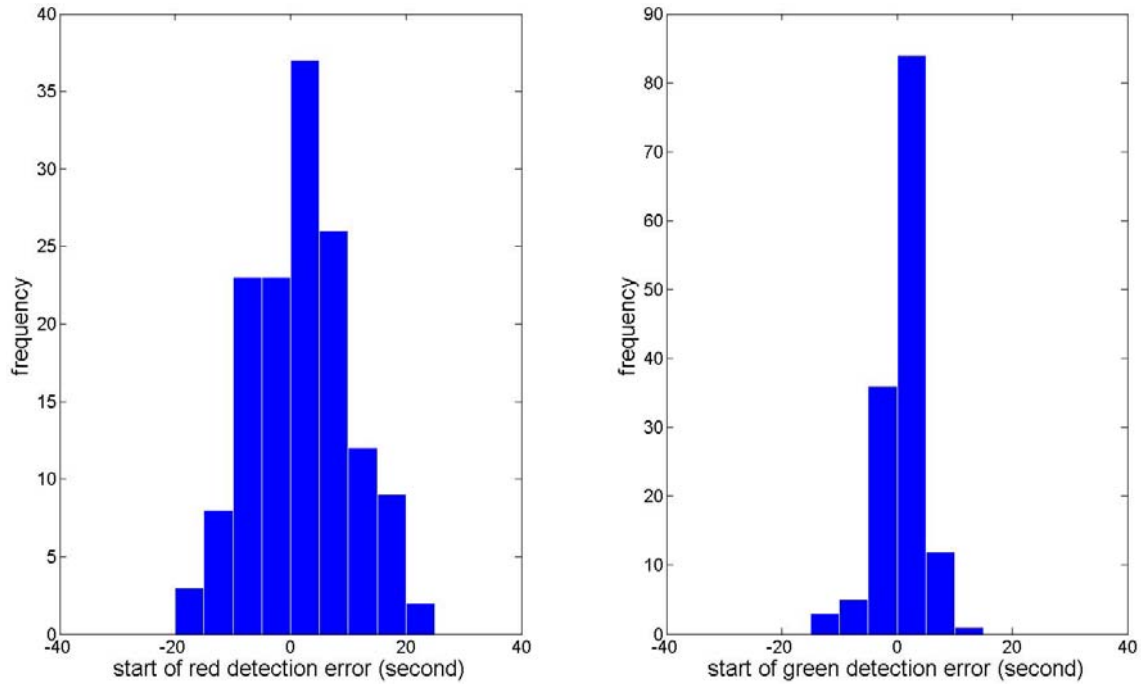
18 The traffic on the link from Intersection 1 to Intersection 2 are studied.
 19 Intersection 1 is the upstream intersection in the case of coordination. There are one
 20 exclusive through lane on the study direction and speed limit is 40 mph. The cycle length
 21 of two intersections is 80 seconds and the green time for the EB traffic is 45 seconds. For
 22 the isolated intersection case, EB traffic do not stop at Intersection 1; for coordinated
 23 mode, the offset of the two signals is 17 seconds which is the free flow travel time. The
 24 demand flow rates have two levels, one is 800 veh/hr/ln for non-peak and the other is
 25 1800 veh/hr/ln for peak hour.

26 The NGSIM (39) data set used in this study are trajectory data on the southbound
 27 link from 11th St to 10th St on Peachtree St. from 4 PM to 4:15 PM. The signal is
 28 coordinated with upstream intersections with a cycle length of 100 seconds. NGSIM has
 29 two sets of arterial data, Peachtree and Lankershim. The Lankershim set has more
 30 measurement errors than the Peachtree set (40), therefore the Peachtree set is chosen.
 31
 32
 33
 34

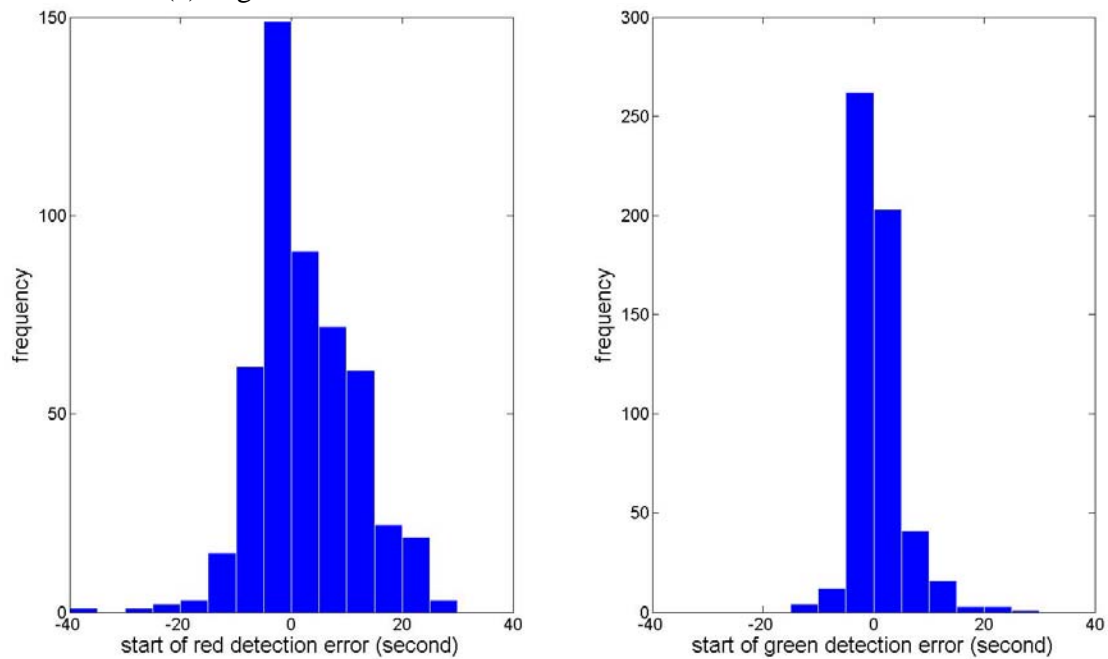
1 **Experiment Results**

2 *Signal Timing Detection*

3 The signal detection results are displayed in Figure 7 and 8. Figure 7 shows the results for
 4 the case of the isolated intersection. Figure 8 shows the results for the case of coordinated
 5 intersections.



(a) Signal Detection for an Isolated Intersection at Non-Peak Hour



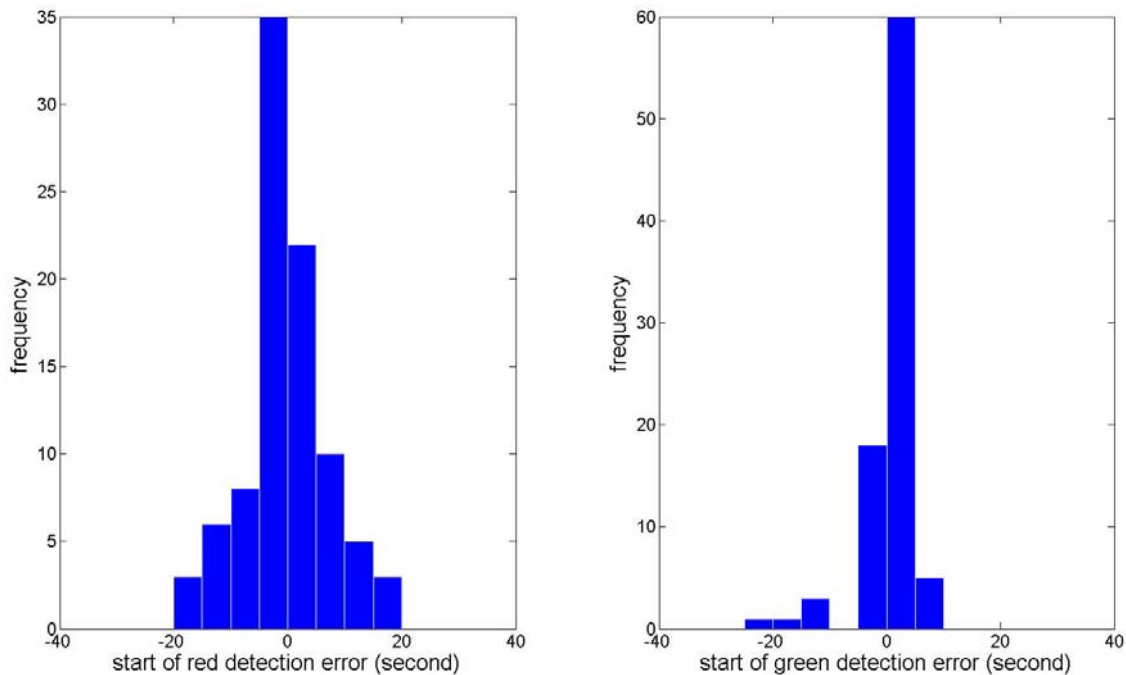
(b) Signal Detection for Isolated Intersection at Peak Hour

FIGURE 7 Signal Detection for an Isolated Intersection

1 Figure 7 shows the results using 15 consecutive cycles' data for each traffic
 2 demand case. The results for the isolated-intersection case are promising. The detected
 3 start times of red and green are quite accurate. The detection of the start of green has
 4 lower errors because the shockwave speed of queue discharging is nearly constant and
 5 traffic in queue discharging usually has fewer disturbances, while the queue formation
 6 shockwave varies more and traffic is "unstable far away"(41). For the peak hour case,
 7 errors distributes similarly to non-peak hour except some "outliers". Further investigation
 8 shows that these "outliers" were from the end of long queues (close to the upstream
 9 intersection) which the traffic is unstable and has more disturbances. By observation,
 10 sometime the shockwaves caused by signal were concealed by the local disturbances and
 11 even human eye has a big difficulty in distinguishing them.

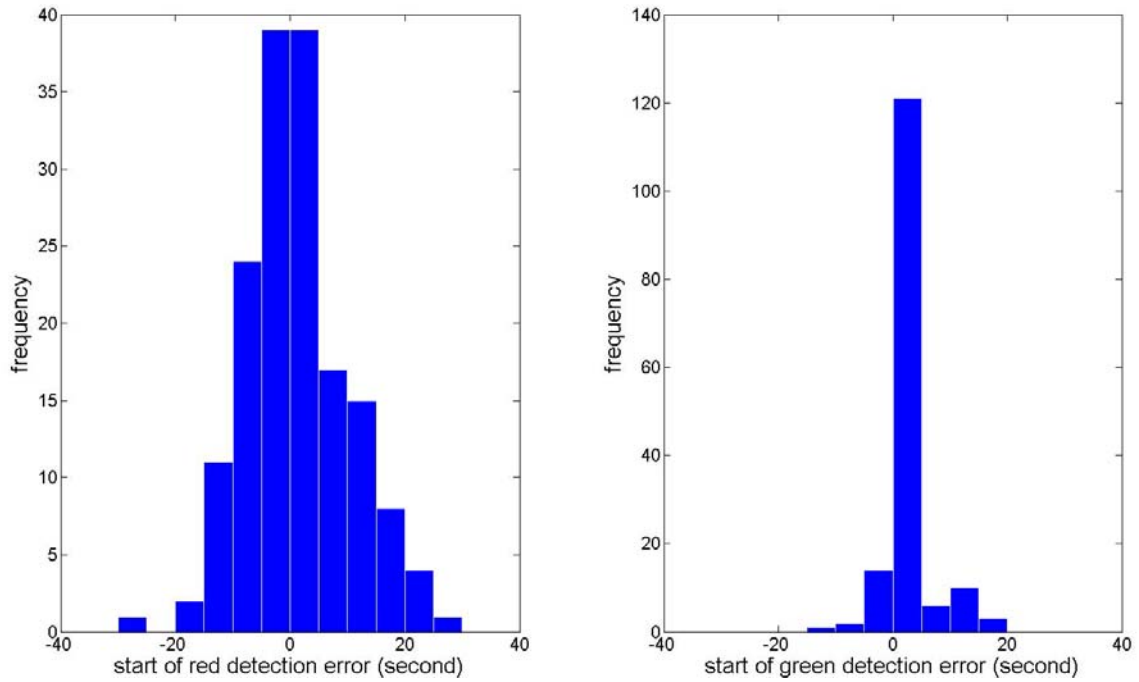
12 Figure 8 shows the results for the case of a coordinated intersection. Figure 8 (a)
 13 and (b) shows the results using 15 consecutive cycle's data for each traffic demand case
 14 and Figure 8 (c) using 10 consecutive cycle's data by NGSIM Figure 8 (a) shows the
 15 results for a non-peak hour case when the coordination is working well. One thing worth
 16 noticing is that there were two cycles when all the vehicles went through the intersection
 17 without significantly slowing down. Hence no available CPs for signal detection were
 18 extracted and therefore the actual timing for the two cycle could not be detected.

19 The overall results indicate that this method gives relatively consistent output for
 20 signal detection.
 21



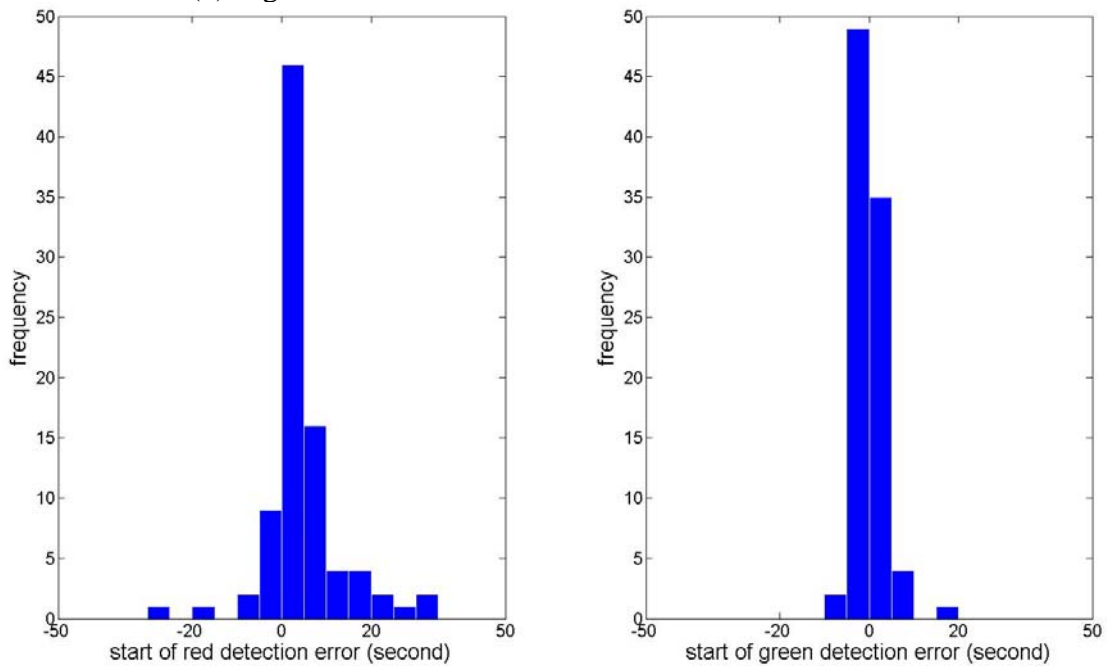
(a) Signal Detection for Coordinated Intersection at Non-Peak Hour

22
 23



1
2

(b) Signal Detection for Coordinated Intersection at Peak Hour



3
4

(c) Signal detection using NGSIM data

FIGURE 8 Detection of Signal Timing for a Coordinated Intersection

5
6
7
8 *Maximum Queue Length Estimation*

9 The performance of the maximum queue length estimation is measured by Mean
10 Absolute Percentage Error (MAPE) which is calculated as:

$$MAPE = \frac{1}{n} \sum_{i=1}^n \left| \frac{GroundTrue - Estimation}{GroundTrue} \right| \times 100\% \quad (18)$$

Where,
 n is the total sample size.

The ground truth queue lengths were collected by observing the overall vehicle trajectories. For the isolated intersection cases, one trajectory was randomly picked for estimation in each cycle. For the coordinated intersection cases as well as NGSIM, three trajectories were randomly picked in each cycle. For each case, experiments were run for 20 times. Table 1 gives the results.

TABLE 1 MAPE of Queue Length Estimation

		# of Cycles	MAPE
SIMU	Isolated (non-peak)	12	18.41%
	Isolated (peak)	12	19.56%
	coordinated (non-peak)	12	22.43%
	coordinated (peak)	12	21.07%
NGSIM	Lane 1*	7	23.35%
	Lane 2**	7	24.16%

* Lane 1 is the lane next to median except left turn lane.

** Lane2 is the lane on the right.

Liu et al. (13) proposed a real-time queue length estimation for congested signalized intersection using the event-based data by SMART-SIGNAL system and the reported MAPE is 14.93%. The results here are comparable to theirs, considering the differences of data resolution. , Since the queue estimation model here is straightforward and serves as a prototype, we expect improved results in future work.

CONCLUSION AND FUTURE STUDY

An innovative approach for arterial intersection performance measurement using vehicle trajectory data is proposed in this paper. To address the challenge of converting the microscopic detections into macroscopic performance measurements, a “critical point” (CP) extraction method is presented. CPs can capture the dynamics of the vehicle and the extraction algorithm has the potential ability for reducing communication cost for onboard GPS devices. Since the extracted CPs represent all the major and minor turbulence and frictions of the vehicle, a CP feature based selection method chooses different types of CPs for difference applications. Using the detected instantaneous end of

1 queue, cycle-by-cycle queue length estimation methods are proposed for both isolated
 2 intersections and intersections with upstream signal impacts. The models are evaluated
 3 by simulated data and the NGSIM trajectory data. The signal timing detection is
 4 relatively accurate except that there are a few start-of-red detection outliers resulting from
 5 stop-and-go flow under oversaturation conditions. The performance of queue length
 6 estimation is also acceptable.

7 Future study will include: 1) the improvement of the CP extraction algorithm and
 8 CP selection design to address the stop-and-go flow; 2) the sensitivity analysis of the
 9 probe data error and sample rate for estimation performance; 3) the adoption of nonlinear
 10 shockwave models which are suitable for arterial traffic flow and are able to support CP
 11 extraction and selection.

12 13 **ACKNOWLEDGEMENT**

14
15 The authors wish to thank all the anonymous reviewers for their valuable comments and
 16 suggestions on this manuscript.

17 18 19 **REFERENCE**

- 20
21 1. Balke, K.N., H. Charara, and R. Parker, *Development of a Traffic Signal*
 22 *Performance Measurement System (Tspms)*. 2005, Texas Transportation Institute.
 23 p. 83.
 24 2. Berkow, M., C.M. Monsere, P.J.V. Koonce, R.L. Bertini, and M. Wolfe.
 25 *Prototype for Data Fusion Using Stationary and Mobile Data Sources for*
 26 *Improved Arterial Performance Measurement*. in *Transportation Research Board*
 27 *88th Annual Meeting*. 2009: Transportation Research Board p.14p.
 28 3. Liu, H.X., W. Ma, X. Wu, and H. Hu, *Development of a Real-Time Arterial*
 29 *Performance Monitoring System Using Traffic Data Available from Existing*
 30 *Signal Systems*. 2008, University of Minnesota, Twin Cities, Minnesota
 31 Department of Transportation. p. 117.
 32 4. Sisiopiku, V.P. and N.M. Roupail, *Toward the Use of Detector Output for*
 33 *Arterial Link Travel Time Estimation: A Literature Review*. Transportation
 34 Research Record, Vol. 1457,1994 pp. 158-165.
 35 5. Zhang, H.M., *Link-Journey-Speed Model for Arterial Traffic*.
 36 TRANSPORTATION RESEARCH RECORD, Vol. 1676,1999 pp. p. 109-115.
 37 6. Zhang, H.M., *Link-Journey-Speed Model for Arterial Traffic*. Transportation
 38 Research Record, Vol. 1676,1999 pp. 109-115.
 39 7. Xie, C., R.L. Cheu, and D.-H. Lee, *Calibration-Free Arterial Link Speed*
 40 *Estimation Model Using Loop Data*. Journal of Transportation Engineering, Vol.
 41 127(6),2001 pp. 507-514.
 42 8. Skabardonis, A. and N. Geroliminis, *Real-Time Monitoring and Control on*
 43 *Signalized Arterials*. Journal of Intelligent Transportation Systems, Vol.
 44 12(2),2008 pp. 64 - 74.
 45 9. Geroliminis, N. and A. Skabardonis, *Prediction of Arrival Profiles and Queue*
 46 *Lengths Along Signalized Arterials by Using a Markov Decision Process*.

- 1 Transportation Research Record: Journal of the Transportation Research Board,
2 Vol. 1934,2005 pp. 116-124.
- 3 10. Viti, F. and H.J. Van Zuylen, *The Dynamics and the Uncertainty of Queues at*
4 *Fixed and Actuated Controls: A Probabilistic Approach*. Journal of Intelligent
5 Transportation Systems, Vol. 13(1),2009 pp. 39-51.
- 6 11. Robinson, S. and J.W. Polak, *Modeling Urban Link Travel Time with Inductive*
7 *Loop Detector Data by Using the K-Nn Method*. Transportation Research Record:
8 Journal of the Transportation Research Board, Vol. 1935,2005 pp. 47-56.
- 9 12. Cheu, R.L., D.-H. Lee, and C. Xie. *An Arterial Speed Estimation Model Fusing*
10 *Data from Stationary and Mobile Sensors*. in *Intelligent Transportation Systems,*
11 *2001. Proceedings. 2001 IEEE*. 2001p.573-578.
- 12 13. Liu, H.X., X. Wu, W. Ma, and H. Hu, *Real-Time Queue Length Estimation for*
13 *Congested Signalized Intersections*. Transportation Research Part C: Emerging
14 Technologies, Vol. 17(4),2009 pp. 412-427.
- 15 14. Liu, H.X., J.S. Oh, S. Oh, L. Chu, and W.W. Recker, *On-Line Traffic Signal*
16 *Control Scheme with Real-Time Delay Estimation Technology*. 2001, Partners for
17 Advanced Transit and Highways (PATH) University of California, Berkeley
18 California Department of Transportation California PATH. p. 15.
- 19 15. Ritchie, S.G., S.-T. Jeng, Y.C. Tok, and S. Park, *Corridor Deployment and*
20 *Investigation of Anonymous Vehicle Tracking for Real-Time Traffic Performance*
21 *Measurement*. 2008, California Partners for Advanced Transit and Highways
22 (PATH), University of California Berkeley, California Department of
23 Transportation. p. 152.
- 24 16. Wilson, R.E. *From Inductance Loops to Vehicle Trajectories*. in *Symposium on*
25 *the Fundamental Diagram: 75 Years (Greenshields 75 Symposium)*. 2008:
26 Transportation Research Board p.11p.
- 27 17. Coifman, B., *Estimating Travel Times and Vehicle Trajectories on Freeways*
28 *Using Dual Loop Detectors*. Transportation Research. Part A: Policy and Practice,
29 Vol. 36(4),2002 pp. 351-364.
- 30 18. Comert, G. and M. Cetin. *Queue Length Estimation from Probe Vehicle Location:*
31 *Undersaturated Conditions*. in *Transportation Research Board 86th Annual*
32 *Meeting*. 2007: Transportation Research Board p.16p.
- 33 19. Hellings, B.R. and L. Fu, *Reducing Bias in Probe-Based Arterial Link Travel*
34 *Time Estimates*. Transportation Research Part C: Emerging Technologies, Vol.
35 10(4),2002 pp. p. 257-273.
- 36 20. Kothuri, S.M., K.A. Tufte, E. Fayed, and R.L. Bertini, *Toward Understanding*
37 *and Reducing Errors in Real-Time Estimation of Travel Times*. Transportation
38 Research Record: Journal of the Transportation Research Board, Vol. 2049,2008
39 pp. 21-28.
- 40 21. Li, Q., T. Miwa, T. Yamamoto, and T. Morikawa. *Some Statistical Properties of*
41 *Arterial Link Travel Time Derived from Historical Probe-Vehicle Data*. in *11th*
42 *World Conference on Transport Research*. 2007: World Conference on Transport
43 Research Society p.34p.
- 44 22. Pan, C., J. Lu, D. Wang, and B. Ran, *Data Collection Based on Global*
45 *Positioning System for Travel Time and Delay for Arterial Roadway Network*.

- 1 Transportation Research Record: Journal of the Transportation Research Board
2 No 2024, Vol.,2007 pp. 35-43.
- 3 23. Liu, H.X., A. Danczyk, R. Brewer, and R. Starr, *Evaluation of Cell Phone Traffic*
4 *Data in Minnesota*. Transportation Research Record: Journal of the
5 Transportation Research Board No 2086, Vol.,2008 pp. 1-7.
- 6 24. Green, M.W., M.D. Fontaine, and B.L. Smith, *Investigation of Dynamic Probe*
7 *Sample Requirements for Traffic Condition Monitoring*. Transportation Research
8 Record, Vol. 1870,2004 pp. 55-61.
- 9 25. Lu, X.-Y. and A. Skabardonis. *Freeway Traffic Shockwave Analysis: Exploring*
10 *Ngsim Trajectory Data*. in *Transportation Research Board 86th Annual Meeting*.
11 2007: Transportation Research Board p.19.
- 12 26. Izadpanah, P., B. Hellinga, and L. Fu. *Automatic Traffic Shockwave Identification*
13 *Using Vehicles' Trajectories*. in *Transportation Research Board 88th Annual*
14 *Meeting*. 2009: Transportation Research Board p.14.
- 15 27. Claudel, C.G., A. Hofleitner, N. Mignerey, and A.M. Bayen. *Guaranteed Bounds*
16 *on Highway Travel Times Using Probe and Fixed Data*. in *Transportation*
17 *Research Board 88th Annual Meeting*. 2009: Transportation Research
18 Boardp.18p.
- 19 28. Daganzo, C.F., *A Variational Formulation of Kinematic Waves: Basic Theory and*
20 *Complex Boundary Conditions*. Transportation Research Part B: Methodological,
21 Vol. 39(2),2005 pp. 187-196.
- 22 29. Newell, G.F., *A Simplified Theory of Kinematic Waves in Highway Traffic, Part I:*
23 *General Theory*. Transportation Research. Part B: Methodological, Vol.
24 27(4),1993 pp. 281-287.
- 25 30. Turner, S.M., W.L. Eisele, R.J. Benz, and D.J. Holdener, *Travel Time Data*
26 *Collection Handbook*. Travel Time Data Collection Handbook. 1998: Texas
27 Transportation Institute, Federal Highway Administration. 348 p.
- 28 31. Levinson, D.M., *Speed and Delay on Signalized Arterials*. Journal of
29 Transportation Engineering, Vol. 124(3),1998 pp. 258-263.
- 30 32. Chen, M. and S. Chien, *Determining the Number of Probe Vehicles for Freeway*
31 *Travel Time Estimation by Microscopic Simulation*. Transportation Research
32 Record, Vol. 1719,2000 pp. 61-68.
- 33 33. *National Traffic Signal Report Card Technical Report 2007*. 2007, Federal
34 Highway Administration, Institute of Transportation Engineers, American Public
35 Works Association, American Association of State Highway and Transportation
36 Officials, ITS America. p. 61.
- 37 34. Ban, X.J., R. Herring, P. Hao, and A. Bayen. *Delay Pattern Estimation for*
38 *Signalized Intersections Using Sampled Travel Times*. in *Transportation Research*
39 *Board 88th Annual Meeting*. 2009. Washington DC21.
- 40 35. Lighthill, M.J. and G.B. Whitham, *On Kinematic Waves. I. Flood Movement in*
41 *Long Rivers*. Proceedings of the Royal Society of London. Series A,
42 Mathematical and Physical Sciences, Vol. 229(1178),1955 pp. 281-316.
- 43 36. Lighthill, M.J. and G.B. Whitham, *On Kinematic Waves. Ii. A Theory of Traffic*
44 *Flow on Long Crowded Roads*. Proceedings of the Royal Society of London.
45 Series A, Mathematical and Physical Sciences, Vol. 229(1178),1955 pp. 317-345.

- 1 37. Richards, P.I., *Shock Waves on the Highway*. operations research, Vol. 4(1),1956
2 pp. 42-51.
- 3 38. Fhwa. *Next Generation Simulation Website*. 2009
4 <http://www.ngsim.fhwa.dot.gov/> Accessed 2009 May 6.
- 5 39. Alexiadis, V., J. Colyar, and J. Halkias, *The Next Generation Simulation*
6 *Program*. ITE Journal, Vol. 74(8),2004 pp. 22-6.
- 7 40. Punzo, V., M.T. Borzacchiello, and B.F. Ciuffo. *Estimation of Vehicle*
8 *Trajectories from Observed Discrete Positions and Next-Generation Simulation*
9 *Program (Ngsim) Data*. in *Transportation Research Board 88th Annual Meeting*.
10 2009: Transportation Research Board p.17.
- 11 41. Smilowitz, K.R., C.F. Daganzo, M.J. Cassidy, and R.L. Bertini, *Some*
12 *Observations of Highway Traffic in Long Queues*. Transportation Research
13 Record, Vol. 1678,1999 pp. 225-233.